Engineering Notes

ENGINEERING NOTES are short manuscripts describing new developments or important results of a preliminary nature. These Notes cannot exceed 6 manuscript pages and 3 figures; a page of text may be substituted for a figure and vice versa. After informal review by the editors, they may be published within a few months of the date of receipt. Style requirements are the same as for regular contributions (see inside back cover).

Compressibility Corrections for Multifoil Sections

Alan Harris*
de Havilland Aircraft of Canada, Ltd.
Toronto, Canada

Introduction

THE calculation of compressible flow about multifoil sections has not developed at the same rate as that for single foils. Flap configurations are generally used at low Mach numbers where the inclusion of viscous effects is somewhat more important than the inclusion of compressibility effects, with the result that the latter is often neglected. The evolution at de Havilland of the transonic multifoil (Fig. 1) from the proven STOL capable augmentor wing[1] has necessitated the parallel development of multifoil compressible methods. To date this has centered around the use of a standard surface singularity potential flow technique that incorporates compressibility by using the Goethert transformation and corrections similar to those developed by Wilby[2] and Labrujere.[3] However, the application of these compressibility corrections to the geometry of Fig. 1 is fraught with difficulty. First, the foils are very thick, typically in the range 18-30%, while the compressibility corrections have been developed for thinner sections. Second, the combination of internal and external flow regions has not been addressed by these methods.

For a number of years, the accepted method for obtaining the compressible flow within a duct has been that due to Lieblein and Stockman (LS).[4] This has been shown to be reliable.[5] However, until recently, it suffered from the absence of a counterpart for external flow and, therefore, could not be applied to general configurations. This deficiency has been remedied by Dietrich, Oehler, and Stockman (DOS),[6] who have modified the internal flow method to produce a compressible flow correction for external flow. Apart from the attraction of now having consistent corrections for all regions of the flow about a general flap configuration, there is also the advantage of them being based on incompressible calculations and, therefore, allowing the combination of solutions.

It is the application of the LS and DOS methods in concert to the geometry of Fig. 1 that is the subject of this paper.

Basic Formulation

It is sufficient here to review the LS and DOS compressibility corrections since Refs. 4 and 6 provide complete details.

The local compressible velocity V_c is obtained as a function of the incompressible velocity V_i from

$$V_c = V_i (\rho_i/\bar{\rho}_c)^{V_i/\bar{V}_i} \tag{1}$$

where $\bar{V}_i$ is the average incompressible velocity, $\bar{\rho}_c$ the average compressible density, and ρ_i the incompressible density equal to the stagnation density ρ_t. The corrections for internal and external flow differ in the definition of $\bar{V}_i$. The internal flow definition is simply the average across the duct. For external flow, the freestream density ratio $(\rho/\rho_t)_\infty$ is used as a weighting factor to average the local incompressible velocity V_i and the freestream incompressible velocity $V_{i,\infty}$ to obtain

$$\bar{V}_i = (\rho/\rho_t)_\infty V_{i,\infty} + [1 - (\rho/\rho_t)_\infty] V_i \tag{2}$$

Modifications to the Basic Formulation

Initial calculations with the DOS external flow compressibility correction indicated that the leading-edge suctions were being overpredicted, while the crest pressures were accurate. This led to the incorporation of a surface slope correction in the definition of $\bar{V}_i$ [Eq. (2)] such that $\bar{V}_i$ is multiplied by $\cos\theta$, where θ is the angle between the local tangent to the surface and the freestream direction (angle of incidence vector). As $\cos\theta$ approaches 0,

$$(\rho_i/\bar{\rho}_c)^{V_i/\bar{V}_i} \to 1.0$$

Therefore, Eq. (1) is well behaved.

The effect of this modification was tested on an 18% thick symmetrical section from Ref. 7. This is the same source as the test case used in Ref. 6, but has a somewhat blunter leading edge and therefore a more peaky pressure distribution. The "exact" compressible flow calculation from Ref. 7 is compared to the DOS correction and the present method, which includes the surface slope correction, in Fig. 2. The agreement near the leading edge and over the aft region of the airfoil is markedly improved. These observations also apply to the test case of Ref. 6 except that, because of the sharper leading edge, the improvement is not as noticeable.

Application to Multifoils

The application of the external flow technique to a single foil or, conversely, the use of the internal flow correction for an isolated duct, is straightforward. Combination of the two methods to calculate the flow about the foil of Fig. 1, which

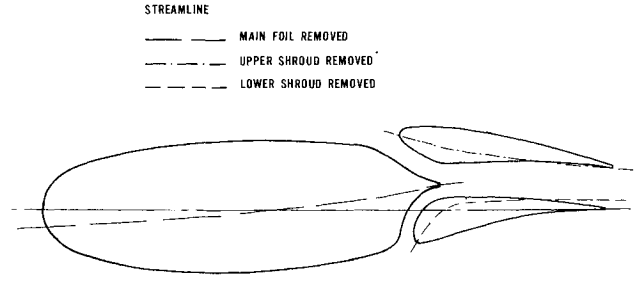

Fig. 1 24% augmentor-wing section, cruise configuration.

Received June 24, 1985; revision received Sept. 27, 1985. Copyright © 1985 by Alan Harris. Published by American Institute of Aeronautics and Astronautics, Inc. with permission.

*Consultant, Augmentor-Wing Group.

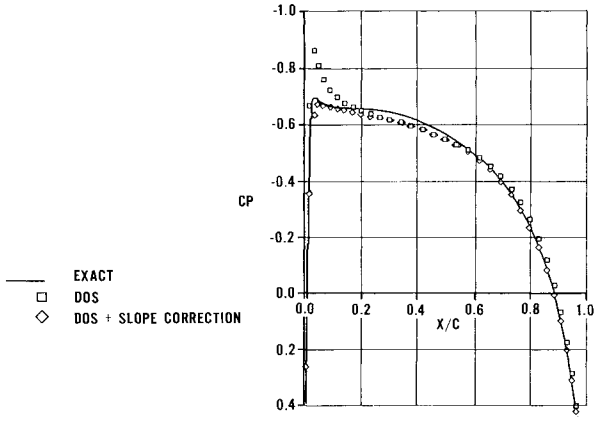

Fig. 2 Effect of slope correction on a symmetrical aerofoil at Mach = 0.6594 and $\alpha = 0$ deg.

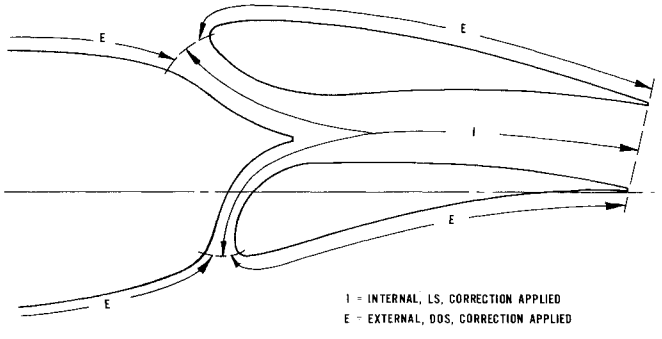

Fig. 3 Application of internal and external corrections.

consists of a main foil and upper and lower shrouds, requires further consideration of the application of the surface slope correction.

As defined, the surface slope is relative to the freestream direction. Within a duct, it is logical to define the stream direction as the axis of the duct. Because the ducts in the multifoil used here have small diffuser angles, the slope correction has not been applied, thus allowing the use of the original formulation of Ref. 4 for the internal flow compressibility correction. It is possible that, for a duct with high contraction or diffusion angles, the slope correction may be necessary.

For the external regions, each foil is in a flowfield created by the freestream and the presence of the other two foils, which implies that the angle of incidence vector is no longer the appropriate stream direction. To allow for this effect on the lower shroud, for example, an inviscid, incompressible calculation of the flow at the appropriate angle of incidence about the main foil and upper shroud (i.e., with the lower shroud removed) provided a streamline in the vicinity of the lower shroud. The angle between the external lower shroud surface and this streamline at a given x/c then gave the value of θ for inclusion in the slope correction. Therefore, each of the foils has an associated streamline that was used for the external correction for that foil. The three streamlines are shown in Fig. 1, with details of the split into internal and external regions being given in Fig. 3. The part of the main foil not shown in Fig. 3 is, of course, an external region.

Exact solutions of the compressible flow around the 24% thick multifoil of Fig. 1 are not available. Therefore, comparisons are presented with experimental results obtained in the NAE 60 × 15 in. two-dimensional wind tunnel. Because of strong viscous effects, especially within the ducts, a boundary layer was incorporated in the calculation using the displacement surface technique. An iterative procedure was used until the predicted displacement surface and the pressure distribution converged.

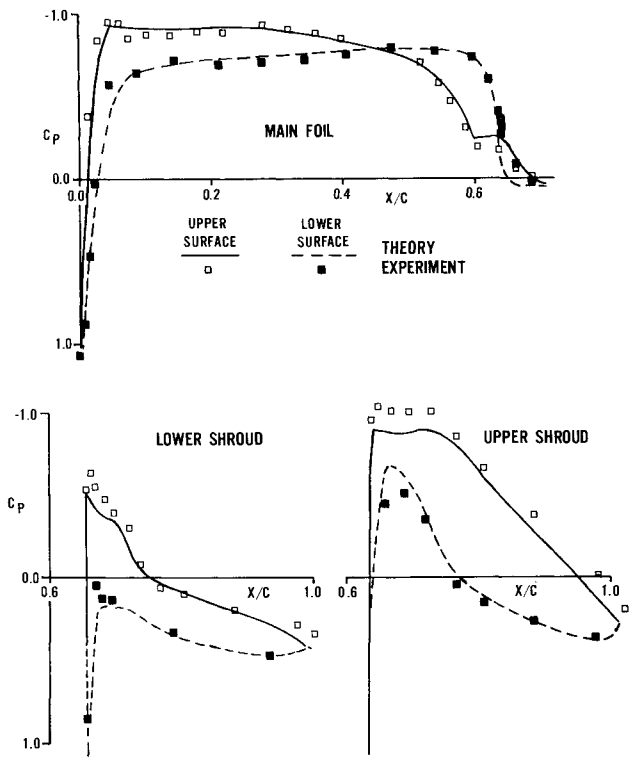

Fig. 4 Theory vs experiment ($M = 0.605$, $C_L = 0.4$).

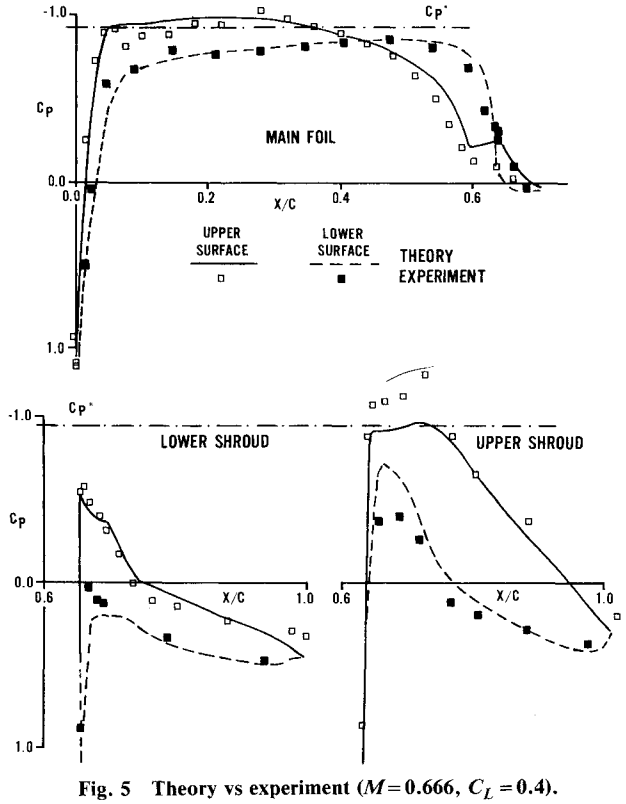

Fig. 5 Theory vs experiment ($M = 0.666$, $C_L = 0.4$).

The comparisons in Figs. 4 and 5 are at $M = 0.605$ and 0.666, respectively, with a lift on the main foil of $C_L = 0.05$ (total C_L was approximately 0.4). The agreement between experiment and theory is very good, especially on the main foil,

and confirms the application of the external compressibility correction to very thick sections. Poorer correlation on the upper shroud upper surface and within the ducts is probably due to the known problem of leakage in Douglas-Neumann surface singularity methods, along with deficiencies in the application of viscous effects producing an incorrect mass flow.

Conclusions

The inclusion of a surface slope correction in the external compressibility correction due to Dietrich, Oehler, and Stockman, has been shown to significantly improve the prediction of compressible velocities. This modified technique for external flow has also been combined with the Lieblein and Stockman compressibility correction for internal flow to produce accurate predictions of the compressible flow around multifoil sections.

Acknowledgment

This work was supported by the Canadian Department of National Defence.

References

[1]Whittley, D. C., "Augmentor-Wing Technology for STOL Transport Aircraft," Paper presented for High Lift Technology Course, University of Tennessee Space Institute, Tullahoma, Oct. 1975.

[2]Wilby, P. J., "The Calculation of Subcritical Pressure Distributions on Symmetrical Aerofoils at Zero Incidence," NPL Aero Rept. 1208, 1967.

[3]Labrujere, Th. E., Loeve, W., and Slooff, J. W., "An Approximate Method for the Calculation of the Pressure Distribution on Wing-Body Combinations at Subcritical Speeds," AGARD CP 71, 1970, pp. 11-0—11-15.

[4]Lieblein, S., and Stockman, N.O., "Compressibility Correction for Internal Flow Solutions," *Journal of Aircraft*, Vol. 9, April 1972, pp. 183-184.

[5]Stockman, N. O., "Potential and Viscous Flow in VTOL, STOL, or CTOL Propulsion System Inlets," AIAA Paper 75-1186, Oct. 1975.

[6]Dietrich, D. A., Oehler, S. L., and Stockman, N. O., "Compressible Flow Analysis About Three-Dimensional Wing Surfaces Using a Combination Technique," AIAA Paper 83-0183, Jan. 1983.

[7]Boerstoel, J. W., "Symmetrical Subsonic Potential Flows Around Quasi-Elliptical Aerofoil Sections," NLR TR 68016, 1968.

Applications of Adaptive-Wall Wind Tunnels

Sanford S. Davis*
NASA Ames Research Center
Moffett Field, California

Introduction

THE purpose of this Note is to introduce a new technique for processing flowfield data from an adaptive-wall wind tunnel. The basic premise is that it may not be necessary, or desirable, to force the adaptive-wall wind tunnel to simulate complete free-air conditions. There are many reasons why this may be an important consideration. For example, the control system in a ventilated wall may not be powerful enough to supply the required inflow/outflow distribution; or a new computer code needs to be validated against an experiment with well-defined, but finite boundary conditions. In three dimensions, the extremely complex mechanical and flow control systems may be an insurmountable barrier to building a facility with complete four-wall active control.

To introduce the method, the concept of a phantom wind tunnel is introduced for both two- and three-dimensional wind tunnels. This is illustrated for a two-dimensional wind tunnel in Fig. 1. The phantom wind tunnel has a solid floor and ceiling and may have an arbitrary height. The height of the phantom wind tunnel is a variable and controllable parameter. The objective is to adapt the walls of the physical wind tunnel in such a manner that the flowfield is equivalent to that in the phantom wind tunnel. By introducing the phantom wind tunnel, a continuous spectrum of flowfields ranging from the original passive and ventilated configuration to the fully adaptive may be obtained.

The three-dimensional phantom wind tunnel must be viewed in a slightly different context. The simplest approximation to three-dimensional wind tunnel interference is to consider an equivalent two-dimensional problem in the far wake or Trefftz plane. This approximation is fully described for subsonic flows in the wall interference literature.[1,2] The equivalent two-dimensional problem is usually solved by an application of the method of images. Such solutions are quite complicated, since a two-dimensional family of images requires doubly infinite summations.

An important limitation of the Trefftz plane analysis is that it does not predict streamwise variations of the interference potential. This shortcoming may be overcome by applying the method of images to the full, three-dimensional configuration. For example, the method of images for a closed-wall, rectangular wind tunnel requires successive rows of upright and inverted image aircraft to satisfy the wall boundary conditions. Consider a wind tunnel with an active floor and celing as shown in Fig. 2. If the flow can be shown to be compatible with that existing between two infinite vertical walls, then the residual interference can be computed with a single array of horizontal images, as depicted in the figure. This flow would be equivalent to a horizontal line of aircraft spaced B units apart and would seem to be a suitable candidate for computation (for a full airplane model) or for analytical studies in the Trefftz plane. In the following sections, two simple examples (in two and three dimensions) are described, followed by a discussion of several possible application areas.

Examples

One method of compatibility assessment for adaptive wall application requires the upwash distribution to be known at two levels in the flow.[3] With respect to the geometrical arrangement depicted in Fig. 3, the two-dimensional algorithm for the case of a cylinder in a wind tunnel follows the following three-step procedure. The upwash v at the selected source level Y_{SL} is measured (or simulated). The next step is to use this source level upwash as a boundary condition to compute a fictitious flow from the source level outward. The domain for this fictitious flow is cross-hatched in Fig. 3. The upwash satisfies a Laplace equation in the case of low-speed or subsonic flows. Whereas conventional adaptive wall algorithms would compute this fictitious flow from Y_{SL} to infinity, the finite domain represented by the phantom wind tunnel allows the physical fluid to be related to the flow in a wind tunnel of semiheight h_{PWT}. The final step is to compare the measured (or simulated) upwash at $y = Y_{FL}$ with that computed from the Laplace equation solution. This comparison is shown in Fig. 4, which shows, as expected, that the flow is not compatible with that in the phantom wind tunnel.

The procedure was repeated once again with a new upwash at Y_{SL}, which simulated the exact analytical solution for

Received March 10, 1985; revision received Oct. 22, 1985. This paper is declared a work of the U.S. Government and therefore is in the public domain.

*Chief, Fluid Dynamics Research Branch. Associate Fellow AIAA.